Published in final edited form as:

Cancer Res. 2020 October 15; 80(20): 4465–4475. doi:10.1158/0008-5472.CAN-20-0789.

Targeting obesity-induced macrophages during preneoplastic growth promotes mammary epithelial stem/progenitor activity, DNA damage and tumor formation

Tamara Chamberlin[1], **Megan Clack**[2], **Caylee Silvers**[2], **Genevra Kuziel**[3], **Victoria Thompson**[2], **Haley Johnson**[2], **Lisa M. Arendt**[1,2,3,*]

[1]Program in Cellular and Molecular Biology, University of Wisconsin-Madison, 1525 Linden Drive, Madison WI 53706

[2]Department of Comparative Biosciences, School of Veterinary Medicine, University of Wisconsin-Madison, 2015 Linden Drive, Madison WI 53706

[3]Program in Cancer Biology, University of Wisconsin-Madison, 1111 Highland Avenue, Madison WI 53705

Abstract

Obesity enhances breast cancer risk in postmenopausal women and premenopausal women with genetic or familial risk factors. We have shown previously that within breast tissue, obesity increases macrophage-driven inflammation and promotes expansion of luminal epithelial cell populations which are hypothesized to be the cells of origin for the most common subtypes of breast cancer. However, it is not clear how these changes within the microenvironment of the breast alter cancer risk and tumor growth. Using a high fat diet to induce obesity, we examined preneoplastic changes associated with epithelial cell-specific loss of Trp53. Obesity significantly enhanced the incidence of tumors of diverse histotypes and increased stromal cells within the tumor microenvironment. Obesity also promoted the growth of preneoplastic lesions containing elevated numbers of luminal epithelial progenitor cells, which were surrounded by macrophages. To understand how macrophage-driven inflammation due to obesity enhances tumor formation, mice were treated with IgG or anti-F4/80 antibodies to deplete macrophages during preneoplastic growth. Unexpectedly, depletion of macrophages in obese mice enhanced mammary epithelial cell stem/progenitor activity, elevated expression of estrogen receptor alpha, and increased DNA damage in cells. Together, these results suggest that in obesity, macrophages reduce epithelial cells with DNA damage, which may limit the progression of preneoplastic breast lesions, and uncovers complex macrophage function within the evolving tumor microenvironment. Understanding how obesity alters the function of macrophages during tumor formation may lead to chemoprevention options for at-risk obese women.

*To whom correspondence should be addressed: Lisa M. Arendt, School of Veterinary Medicine, 2015 Linden Drive Rm 4354A, Madison, WI 53706, Phone: (608) 890-2265; Fax: (608) 263-3926, lmarendt@wisc.edu.

Conflict of Interest Statement: The authors have no potential conflicts of interest to declare.

Keywords

obesity; breast cancer; macrophage; trp53; stem cells

INTRODUCTION

Obesity has nearly tripled worldwide since 1975 with over 650 million adults classified as obese in 2016 (1). Obesity is a significant risk factor for breast cancer in postmenopausal and high-risk premenopausal women (2,3). Regardless of menopausal status, obesity is associated with higher breast cancer-associated mortality rates (4). Understanding how obesity impacts early breast cancer progression may result in improved chemoprevention strategies or weight loss interventions to decrease breast cancer risk.

The breast epithelium and surrounding stroma undergo changes in obesity. Luminal epithelial cells expressing estrogen receptor alpha (ERα) and those with stem/progenitor activity are increased in obese women and mice fed a high fat diet (HFD) to induce obesity (5). Current hypotheses suggest that transformation of luminal progenitor cells may lead to the most common types of breast cancer (6,7). However, little is known about how obesity-induced alterations in stem/progenitor cells may impact tumor incidence or subtypes of tumors that form. Within the breast stroma in obesity, inflammatory macrophages are recruited to remove dead adipocytes, forming characteristic crown-like structures (8). Within normal breast tissue, macrophages play a role in regulating epithelial stem/progenitor cells (9,10). In preneoplastic lesions, macrophages promote mammary tumor progression and metastasis (11,12) and have become a clinical focus for cancer therapy and chemoprevention (13). However, the role of macrophages in early tumor progression in obesity has been unexplored.

TP53 is one of the most frequently mutated or deleted genes in breast cancer and has been found inactivated in all breast cancer subtypes (14). Obese breast cancer cases are also more likely to have TP53 mutations (15). TP53 functions as a tumor suppressor gene, and p53 plays a central role in cell cycle arrest and DNA damage repair pathways. Mice transplanted with $p53^{-/-}$ mammary epithelial cells (MECs) develop diverse subtypes of carcinomas (16,17). Further, mice transplanted with $p53^{-/-}$ MEC develop hyperplasias and ductal carcinoma in situ that are $ER\alpha^{+}$ and hormonally responsive prior to formation of $ER\alpha^{+}$ or $ER\alpha^{-}$ tumors (18). Changes in the mammary microenvironment alters the histotypes of resulting tumors (19), suggesting that alterations caused by obesity may impact $p53^{-/-}$ mammary tumor growth.

Here, we investigated how obesity alters $p53^{-/-}$ mammary tumor development and progression. We show that obesity significantly increased incidence of mammary tumor formation with enhanced recruitment of tumor stroma. Preneoplastic changes occurred frequently in obese mice, with expansion of luminal epithelial cell populations with increased stem/progenitor activity and enhanced DNA damage. Strikingly, depletion of macrophages uncovered a unique, protective role for macrophages in limiting DNA damage and reducing stem/progenitor cells within the obese mammary microenvironment.

MATERIALS AND METHODS

Animal Models

Animal procedures were performed with an approved protocol from the University of Wisconsin-Madison IACUC. Mice were housed in AAALAC-accredited facilities. FVB/N female mice were purchased from Taconic Biosciences (FVB/NTac; RRID:MGI:3528175). Trp53 mice were obtained from Dr. Eric Sandgren and backcrossed onto the FVB/N genetic background for 10 generations. Genotyping was performed by Transnetyx. All mice were given food and water *ad libitum*.

Mammary Epithelial Cell Transplants

MECs were isolated from 6–8 week-old $Trp53^{-/-}$ female mice (5), and 400,000 MECs were suspended in 50/50 Matrigel (Corning, 354234) and DMEM:F12 media and transplanted into inguinal mammary glands of 3-week-old female mice that were cleared of endogenous MECs (7). Recipient mice were randomized to receive low-fat (LFD; 6.2% kcal from fat; Teklad Global #2018) or high-fat (HFD; 60% kcal from fat; Test Diet #58126) purified diets that contained equal amounts of vitamins and micronutrients. Mice were weighed weekly, and the initial weight was subtracted from the measured weight. Mammary glands were collected from diestrus-staged mice at 8 weeks after transplant or at end stage when tumors reached 1.5 cm in diameter or mice reached 1 year of age without tumor formation (Figure S1A, B). Diestrus was determined using vaginal cytology (5). One hour prior to euthanasia, mice were injected with 200 mg/kg 5-Bromo-2′-deoxyuridine (BrdU; Fisher Scientific, ICN10017101) diluted in PBS.

Macrophage Depletion

Four weeks following transplant, mice in each diet group received subcutaneous injections of antibodies (Figure S1C), as described (20). Mice received a loading dose of 400 μg of rat IgG2b isotype (BioXCell, BE0090; RRID:AB_1107780) or InVivoMAb anti-mouse F4/80 (BioXCell, BE0206; RRID:AB_10949019) antibodies followed by injections of 200 μg every 48 hr for 4 weeks.

Flow Cytometry and Progenitor Assays

MECs were lineage-depleted utilizing anti-CD31 (0.5mg/mL,102401; RRID:AB_312896), anti-TER-119 (0.5mg/mL,116201; RRID:AB_313702), and anti-CD45 (0.5mg/mL, 103102; RRID:AB_312967) antibodies (Biolegend) conjugated to sheep anti-rat IgG Dynabeads (Invitrogen, 11035). Lineage-depleted cells were stained with Ghost Violet 450 viability dye (TONBO Biosciences, 13–0863-T100). For immunotyping, MECs were incubated with CD16/32 antibodies (ThermoFisher; 14–0161-82; RRID:AB_467133), followed by fixable viability dye eFluor 780 (eBiosciences; 65–0865). Antibodies are listed in Table S1. Cells were analyzed using BD LSR Fortessa (BD Biosciences). Immune cells were identified as described (21). Gates were set on fluorescence minus one controls, and data were analyzed using FlowJo software (TreeStar V10; RRID:SCR_008520). Progenitor assays were conducted as described (5).

Histological Classification

Mammary glands and tumors were fixed in 10% formalin and stained with hematoxylin and eosin (H&E) by UWCCC Experimental Pathology Laboratory. Tumor sections were blinded then classified based on cellular morphology and arrangement. Hyperplastic ducts contained 3 or more layers of MECs, and 10 ducts/gland were analyzed. Adipocyte diameters were measured from 10 adipocytes/image on 5 images/mouse. Crown-like structures were quantified using tissue sections stained with anti-F4/80 antibodies (Biolegend; 157301; RRID:AB_2814089) (5). Immunohistochemistry and immunofluorescence were conducted with antibodies in Table S1 as described (5).

Other Methods

Expanded methods are provided in Supplemental Methods. Primer sequences for quantitative RT-PCR are provided in Table S2.

Statistical Analyses

Results were expressed as the mean ± s.e.m., unless stated. Statistical differences between 2 groups was determined using Student's t test and among more than 2 groups using one-way analysis of variance (ANOVA) with Tukey's multiple comparison posttest. Differences in groups with two variables were determined using two-way ANOVA. *P* values of 0.05 or less were considered significant. Statistical analyses were conducted using GraphPad Prism 8.0.3 (GraphPad Software; RRID:SCR_002798).

RESULTS

Obesity increased incidence of $p53^{-/-}$ mammary tumors and enhanced tumor stroma

To examine how obesity altered mammary tumor formation, MECs were isolated from $Trp53^{-/-}$ mice and transplanted into epithelium-free mammary fat pads of 3-week-old non-transgenic female mice (22). Following transplant, mice were fed either LFD or HFD, as we have shown (5). HFD-fed mice gained significantly more weight than LFD-fed mice 4 weeks following transplant (Figure 1A). HFD-fed mice had a mild, but significant decrease in mammary tumor-free survival (P=0.04, Figure 1B). Of the 12 LFD-fed transplanted mice, 7 mice formed 1 mammary tumor each. Strikingly, of the 19 HFD-fed transplanted mice, 18 mice developed 25 mammary tumors with significantly increased incidence compared to LFD-fed mice (P=0.009, Fisher's exact test).

To identify the impact of obesity on tumor histotypes, $p53^{-/-}$ tumors were classified based on cell morphology and pattern formation (Figure 1C). Similar to other studies of $p53^{-/-}$ tumorigenesis in the FVB/N genetic background (23,24), the most common histotype observed was spindle cell carcinomas, which formed at similar rates in LFD and HFD-fed mice (Figure 1C). Adenocarcinomas also formed at a similar rate between groups. However, the HFD-fed group developed a small number of more diverse carcinoma histotypes including solid carcinomas, a squamous cell carcinoma and a mucinous carcinoma. The tumors that formed in both groups demonstrated variable expression of luminal marker cytokeratin 8 (CK8), basal/myoepithelial marker cytokeratin 5 (CK5), and ERα (Figure S2A, B, C). Regardless of histotype, we observed significantly higher expression of

proliferation marker Ki67 in $p53^{-/-}$ carcinomas that formed in HFD-fed mice compared to those fed LFD (P=0.005; Figure 1D), although overall tumor growth rates were not significantly different (Figure S2D). Together, these results suggest that obesity increases the incidence of mammary tumor formation but does not alter the spectrum of histotypes of resulting tumors.

Within mammary adipose tissue of non-tumor-bearing mice, obesity significantly enhances recruitment of macrophages (5,25). We hypothesized that obesity would also enhance macrophage recruitment within the tumor microenvironment. Within tumors, the number of $F4/80^{+}$ macrophages varied among tumor histotypes with the lowest infiltration observed within adenocarcinomas (Figure S2E). Spindle cell carcinomas from HFD-fed mice demonstrated significantly increased macrophage recruitment compared to those from LFD-fed mice (P=0.05, Figure 1E). Consistent with increased collagen deposition within the breast tumors of obese women (26), we also observed a significant increase in collagen within tumors from HFD-fed mice compared to those from LFD-fed mice (P=0.02, Figure 1F). These results suggest that obesity promotes the recruitment of macrophages into the tumor microenvironment and enhances collagen deposition.

Obesity enhanced formation of ductal hyperplasias with increased macrophage infiltration

To examine early tumor formation, we collected mammary glands prior to evidence of tumors at 8 weeks following $p53^{-/-}$ MEC transplantation. At this time point, HFD-fed mice demonstrated significantly increased weight gain (Figure 2A), resulting in significantly larger mammary adipocytes (P=0.03, Figure 2B) and formation of $F4/80^{+}$ crown-like structures (P=0.006, Figure 2C). These results suggest that inflammatory changes associated with obesity occur concurrently with weight gain.

Examination of the mammary epithelium revealed that a significantly greater percentage of ducts in the mammary glands of HFD-fed mice had hyperplastic epithelium compared to those from LFD-fed mice (P=0.002, Figure 2D). To identify how hyperplasias developed over time, we examined transplanted mammary glands from LFD and HFD-fed mice that developed tumors in the opposite mammary gland. At 100 and 200 days following $p53^{-/-}$ MEC transplant, the percentage of mammary ducts with hyperplastic epithelium remained significantly higher in HFD-fed mice compared to controls (Figure 2E). At 8 weeks following transplant, $p53^{-/-}$ MECs within ducts of HFD-fed mice expressed significantly higher Ki67 expression compared to those from LFD-fed mice (P=0.004, Figure 2F), suggesting that obesity promotes epithelial cell proliferation.

Consistent with increased crown-like structures within adipose tissue of HFD-fed mice, we also observed increased $F4/80^{+}$ macrophages surrounding and interdigitating between MECs of ducts (P=0.004, Figure 2G). Compared to those from LFD-fed mice, $F4/80^{+}$ macrophages isolated from transplanted mammary glands of HFD-fed mice expressed significantly higher levels of inflammatory cytokines *Il6* and *Tnf*, as well as *Cd11c* (Figure 2H), consistent with macrophages from obese visceral fat (27). Macrophages from HFD-fed mice also expressed elevated levels of *Cd36* and *Plin2* (Figure 2H), which may reflect increased lipid metabolism (27). Obesity also enhances collagen deposition within mammary adipose tissue (26). We observed increased collagen surrounding the mammary ducts of HFD-fed mice compared to

controls (P=0.0009, Figure 2I). These results suggest that obesity promotes the early growth of preneoplastic lesions with enhanced stromal development.

Obesity increased p53$^{-/-}$ MEC progenitor activity 8 weeks following transplant

We have shown that obesity alters MEC populations in non-tumor-bearing mice leading to enhanced numbers of luminal progenitor cells (5). To examine how obesity alters p53$^{-/-}$ MEC populations prior to tumor formation, we isolated MECs 8 weeks following transplantation. Lineage-depleted MECs were stained with antibodies for EpCAM, CD49f, CD49b, and Sca-1. Epithelial cells were gated to identify EpCAM^{hi}CD49f^{lo} luminal cells and EpCAM^{lo}CD49f^{hi} basal cells (Figure 3A, Figure S3A). When compared to MECs from LFD-fed mice, the ratio of luminal to basal p53$^{-/-}$ MECs was significantly increased in HFD-fed mice (P=0.01; Figure 3A). No significant differences were observed in EpCAM^{-}CD49f^{-} stromal cells or EpCAM^{-}CD49f^{+} cells (Figure S3B, S3C). The luminal cells were further gated into Sca-1^{+}CD49b^{-} ERα^{+} cells, Sca-1^{+}CD49b^{+} ERα^{+} progenitor cells, and Sca-1^{-}CD49b^{+} ERα^{-} cell populations (28). ERα^{+} luminal progenitor cells were significantly increased in the mammary glands of HFD-fed mice (P=0.05; Figure 3A), while no significant differences were observed in either of the other luminal cell populations compared to controls (Figure S3D).

To identify changes in epithelial cell populations within the tissue, we examined MEC expression of CK8 and CK5 within transplanted mammary glands. Within the ducts of HFD-fed mice, CK8^{+} cells were enriched and CK5^{+} cells were reduced, resulting in decreased continuity of CK5^{+} cells surrounding the ducts compared to controls (P=0.04, Figure 3B). In the hyperplastic ducts of both LFD and HFD-fed mice, a small number of CK8 and CK5 co-labeled cells were identified (Figure 3C). Within the luminal layer, we also observed a significant increase in the percentage of ERα^{+} cells within the ducts of HFD-fed mice (P=0.001, Figure 3D). In both mice and humans, rare ERα^{+} cells have been identified that co-label with markers of proliferation (29), suggestive of ERα^{+} progenitor cells (30). We also observed a significant increase in the percentage of cells that co-labeled for ERα and proliferation marker, BrdU (P=0.03, Figure 3E). Together, these results suggest that obesity enhances p53$^{-/-}$ ERα^{+} luminal cells and decreases basal/myoepithelial cells prior to tumor formation.

With these observed changes in cell populations, we hypothesized that obesity may also enhance stem/progenitor activity within the transplanted p53$^{-/-}$ MECs. To examine stem/progenitor activity, we isolated p53$^{-/-}$ MECs and plated cells in mammosphere and colony forming assays. Isolated p53$^{-/-}$ MECs from HFD-fed mice formed significantly higher numbers of both primary and secondary mammospheres compared to those from LFD-fed mice (Figure 3F). Although we observed increased mammosphere formation in p53$^{-/-}$ MECs from HFD-fed mice, no differences were observed in mammosphere size in either primary or secondary mammospheres compared to controls (Figure 3F). Isolated p53$^{-/-}$ cells from HFD-fed mice generated significantly increased numbers of colonies compared to those from LFD-fed mice (P=0.02, Figure 3G). The colonies that formed expressed CK8 and demonstrated variable cell arrangement, with some round colonies containing luminal cells surrounded by CK14^{+} basal cells and others with luminal and basal cells throughout the

colonies. These results indicate that obesity significantly increases $p53^{-/-}$ epithelial cell progenitor cells prior to tumor formation.

Macrophage depletion enhanced stem/progenitor activity 8 weeks following transplant in obese mice

Macrophages have been shown to enhance the progression of preinvasive mammary lesions (11,12), and we hypothesized that macrophages may promote tumor progression in obesity. To investigate this hypothesis, $p53^{-/-}$ MECs were transplanted into mammary fat pads of recipient mice, and mice were randomized to receive either LFD or HFD. Four weeks following transplantation, mice in each group received either IgG or anti-F4/80 (aF4/80) antibodies for an additional 4 weeks (Figure 4A). Treatment with aF4/80 antibodies did not significantly alter weight in either HFD or LFD groups (Figure 4B). To confirm macrophage depletion, we examined $F4/80^{+}$ macrophages using antibodies that detected a different epitope of the F4/80 protein. Mice treated with aF4/80 antibodies in both diet groups had significantly decreased numbers of macrophages surrounding mammary ducts and interdigitating between MECs compared to those treated with IgG (Figure 4C). The percentage of ducts containing macrophages interdigitating between MECs was significantly decreased in mice treated with aF4/80 antibodies in both groups compared to those treated with IgG (Figure 4D).

To examine changes in immune cell populations that might occur in response to depletion of macrophages, we isolated cells from transplanted mammary glands of IgG or aF4/80-treated HFD-fed mice and examined immune cell populations using flow cytometry (Figure S4A). No significant differences were observed in $CD45^{+}$ immune cells in mammary glands of IgG and aF4/80-treated mice (Figure S4B). Consistent with depletion of macrophages, we observed a significant decrease in $CD11b^{+}$ myeloid lineage cells in mammary glands from aF4/80-treated mice compared to IgG-treated mice (P=0.05; Figure S4C). However, no significant differences were observed in $CD11b^{+}Ly6G^{+}$ neutrophils, $CD11b^{+}CD24^{+}$ IA/IE^{-} eosinophils or $CD11b^{+}CD24^{+}IA/IE^{+}$ dendritic cells within the $CD11b^{+}$ cell population from mice in either group (Figure S4D). Together these results suggest that treatment with aF4/80 antibodies significantly reduced macrophages without significantly depleting other myeloid lineage cell types.

To examine the effects of macrophage depletion on preneoplastic growth, we quantified hyperplastic ducts within the mammary glands of mice in each treatment group. HFD-fed mice demonstrated significantly increased numbers of ductal hyperplasias compared with LFD-fed mice (Figure 4E). However, macrophage depletion did not significantly reduce the number of hyperplastic ducts in either LFD or HFD-fed mice compared with their respective IgG-treated controls (Figure 4E).

Macrophages have been shown to regulate mammary stem/progenitor cells in non-tumor-bearing mice (9,10). To examine the effect of macrophage depletion on $p53^{-/-}$ MEC stem/progenitor activity, we isolated MECs from treated mice and quantified mammosphere formation. Isolated $p53^{-/-}$ MECs from IgG-treated HFD-fed mice formed significantly higher numbers of both primary and secondary mammospheres compared to those isolated from both groups of LFD-fed mice (Figure 4F). Depletion of macrophages in LFD-fed mice

did not significantly alter primary or secondary mammosphere formation compared to IgG-treated LFD-fed mice (Figure 4F). Unexpectedly, depletion of macrophages in HFD-fed mice resulted in significantly increased primary and secondary mammospheres compared to IgG-treated HFD-fed mice ($P<0.0001$, Figure 4F). These results suggest that macrophages reduce stem/progenitor activity in $p53^{-/-}$ MECs from obese mice.

To understand the effects of macrophage depletion on epithelial cells within the mammary glands, we quantified the percentage of $ER\alpha^+$ MECs. IgG-treated HFD-fed mice demonstrated a significantly increased percentage of $ER\alpha^+$ MECs compared to both groups of LFD-fed mice (Figure 4G). Depletion of macrophages in LFD-fed mice did not significantly alter $ER\alpha^+$ MECs compared to IgG-treated LFD-fed mice (Figure 4G). In contrast, depletion of macrophages in HFD-fed mice resulted in a significant increase in $ER\alpha^+$ MECs compared to IgG-treated HFD-fed mice ($P<0.0001$, Figure 4G). When $p53^{-/-}$ MECs were co-labeled with ERα and BrdU, we observed a significant increase in $ER\alpha^+BrdU^+$ MECs of IgG-treated HFD-fed mice compared with LFD-fed mice in either group (Figure 4H). Depletion of macrophages in LFD-fed mice did not significantly alter the number of $ER\alpha^+BrdU^+$ cells compared to IgG-treated controls (Figure 4H). Depletion of macrophages in HFD-fed mice significantly enhanced $ER\alpha^+BrdU^+$ MECs compared to IgG-treated HFD-fed mice ($P=0.002$, Figure 4H). These results suggest that macrophages reduce $ER\alpha^+$ proliferating cells within mammary glands in obesity.

Macrophage depletion in obese mice increased cells with DNA damage

TP53 plays an important role as a tumor suppressor through regulation of multiple DNA repair pathways (31), and obesity has been linked to genomic instability in diverse cell types (32). To examine how obesity impacted DNA damage, we performed comet assays to examine single and double strand DNA breaks. Isolated $p53^{-/-}$ MECs from donor mice were grown for 7 days in culture and treated with H_2O_2 to induce oxidative damage. H_2O_2-treated cells demonstrated significantly increased percent DNA in tails and olive moment compared to vehicle-treated cells (Figure S5A). Consistent with elevated DNA damage, H_2O_2-treated $p53^{-/-}$ MECs expressed higher levels of the phosphorylated form of histone H2A variant H2AX, γH2AX (Figure S5B), which has been identified as a marker of DNA double-stranded breaks (33). To assess DNA damage *in vivo*, we isolated $p53^{-/-}$ MECs 8 weeks following transplantation from LFD and HFD-fed mice. Transplanted $p53^{-/-}$ MECs isolated from IgG-treated HFD-fed mice demonstrated significantly increased DNA damage compared to both groups of LFD-fed mice (Figure 5A). While no differences were observed in DNA damage between LFD-fed groups (Figure 5A), MECs from aF4/80-treated HFD-fed mice had significantly increased percent DNA in tail and olive moments compared to IgG-treated HFD-fed mice (Figure 5A).

Because replicating cells in S-phase express γH2AX constitutively (34,35), we co-labeled transplanted $p53^{-/-}$ MECs for BrdU and γH2AX. IgG-treated HFD-fed mice demonstrated significantly increased numbers of BrdU labeled cells compared to IgG-treated LFD-fed mice ($P=0.04$, Figure 5B), although no significant difference was observed in the percentage of γH2AX expressing cells (Figure S5C). No significant differences were also observed between IgG and aF4/80-treated LFD-fed mice for either BrdU labeling (Figure 5B) or

γH2AX expression (Figure S5C). However, depletion of macrophages in HFD-fed mice significantly reduced BrdU labeled cells compared to IgG-treated HFD-fed mice (P=0.001, Figure 5B) and significantly increased γH2AX expression (P=0.02, Figure S5C). γH2AX $^{+}$BrdU^{-} p53$^{-/-}$ MECs were significantly increased in aF4/80-treated HFD-fed mice compared to IgG-treated HFD-fed mice (P<0.0001, Figure 5C). Together, these results suggest that macrophage depletion in obese mice increases p53$^{-/-}$ MECs with double-strand DNA breaks.

Oxidative stress caused by extracellular and intracellular production of reactive oxygen species leads to damage of nucleic acids that can cause DNA strand breaks (36). To examine oxidative stress, we quantified labeling for 8-hydroxy-2'-deoxy guanosine (8-OHdG), a marker for endogenous oxidative DNA damage (37). Significantly increased 8-OHdG labeling was detected in p53$^{-/-}$ MECs from IgG-treated HFD-fed mice compared to IgG-treated LFD-fed mice (P=0.03, Figure 5D). No significant differences in 8-OHdG labeling were detected between LFD-fed groups (Figure 5D). However, HFD-fed macrophage-depleted mice demonstrated significantly increased 8-OHdG labeling compared to all other treatment groups (Figure 5D). These results suggest that oxidative DNA damage is increased in p53$^{-/-}$ MECs in obese mice and is significantly increased with macrophage depletion.

Consistent with increased markers of DNA damage, 2 out of 9 of the macrophage-depleted HFD-fed mice developed spindle cell carcinomas 8 weeks after transplant, while mice in all other treatment groups remained mammary tumor-free at this timepoint (P=0.06, chi-squared test for trend; Figure 5E). Together, these results suggest that macrophages reduce p53$^{-/-}$ MECs with DNA damage within obese mammary glands, which may have a protective role against tumor formation.

DISCUSSION

Obesity results in increased adipocyte hypertrophy and death, leading to a state of chronic, macrophage-driven inflammation (8). We observed early evidence of crown-like structures within obese fat, which have been associated with increased risk of breast cancer following diagnosis of benign breast disease (38). Macrophages have been shown to enhance progression of preneoplastic mammary lesions and promote early metastatic dissemination (11,12), and we observed that depletion of macrophages surrounding preneoplastic lesions led to significantly reduced p53$^{-/-}$ MEC proliferation in HFD-fed mice. These results suggest that macrophages could enhance growth of preneoplastic lesions through secretion of inflammatory cytokines or direct interactions with MECs (39). However, we uncovered a critical role for macrophages in reducing cells with DNA damage in obesity. Depletion of macrophages in obese mice led to increased p53$^{-/-}$ MECs exhibiting stem/progenitor activity and DNA damage. We also observed early development of mammary tumors in a subset of obese mice receiving aF4/80 antibodies, which suggests that elevated DNA damage may enhance tumor formation. Given the interest in macrophages as a clinical target for breast cancer therapeutics and chemoprevention (40), this surprising finding may suggest that strategies to reduce macrophages or alter their function following a diagnosis of early breast disease may not benefit obese patients.

During tumor formation, $p53^{-/-}$ MECs proceed through hormonally sensitive, $ER\alpha^{+}$ preneoplastic lesions prior to the development of $ER\alpha^{+}$ or $ER\alpha^{-}$ mammary tumors. Although we observed that obesity enhanced $ER\alpha^{+}$ progenitor cell populations during preneoplastic growth, the resulting tumor histotypes were similar to those observed in control mice, suggesting that the microenvironment induced by obesity did not select for specific types of tumors. Interestingly, our data suggest that macrophages reduce $ER\alpha^{+}$ cells and epithelial stem/progenitor activity during this early stage of tumor formation in obesity. This may be an effect of macrophage secreted cytokines, as conditioned media from macrophages has been shown to reduce ERα expression in MCF-7 and T47D breast cancer cell lines (41). In hyperplasias of obese mice, luminal epithelial cells were significantly increased with a concurrent decrease in basal/myoepithelial cells. Depletion of macrophages in obese mice further enhanced $ER\alpha^{+}$ MECs, however, the resulting tumors that formed were spindle cell carcinomas, a subtype with similarities to the claudin-low molecular subtype in breast cancer patients (17). A recent study of tumorigenesis in the Trp53/$BRCA1^{-/-}$ mouse model suggests that inadequate DNA damage repair is an underlying mechanism for the acquisition of mesenchymal characteristics within luminal MECs (42). During tumorigenesis in $p53^{-/-}$ MECs, we observed a population of cells in hyperplasias of both obese and control mice that expressed both luminal and basal markers. It is tempting to speculate that progenitor cells for luminal lineages may contribute to the formation of claudin-low tumors through a similar mechanism of inadequate DNA repair in $p53^{-/-}$ MECs. Further studies are necessary using lineage-tracing approaches to understand how different stem/progenitor populations may contribute to the histotypes observed during $p53^{-/-}$ tumorigenesis.

In obese individuals, a broad range of DNA lesions including double strand breaks, single strand breaks, and oxidized DNA bases, such as 8-OHdG, have been observed in multiple cell types (32). We observed evidence of increased single and double strand DNA breaks in $p53^{-/-}$ MECs isolated from obese mice. Oxidative stress, caused by intracellular and extracellular overproduction of reactive oxygen species, leads to the formation of DNA adducts and strand breaks that can result in mutations leading to cancer (43). Since TP53 mutations are increased in breast tumors of obese patients (15), it is possible that elevated oxidative stress plays a role in this increased mutation rate. While macrophages produce reactive oxygen species (44), macrophage depletion in obese mice led to significantly enhanced DNA damage as measured through comet assays and expression of 8-OHdG and γH2AX. These results suggest that macrophages reduce DNA damage in the context of obesity. Since elevated free fatty acids enhance oxidative stress (45), macrophages could indirectly reduce oxidative damage in the obese microenvironment by scavenging lipids from necrotic adipocytes within crown-like structures (27). Macrophages may also have more direct effects on DNA damage repair in epithelial cells. Recently, macrophages have been shown to reduce the number of cells with double strand breaks by secreting HB-EGF to enhance homologous recombination in surrounding DNA-damaged cells (46). Understanding how macrophages reduce epithelial cell DNA damage in obesity is necessary for developing therapeutics to target macrophages in obese patients.

Women diagnosed with benign breast disease, family history of breast cancer or underlying genetic risk factors may be ideal candidates for chemoprevention strategies to reduce risk for

breast cancer formation. Weight loss is clinically recommended for obese individuals however, it is currently unknown how weight loss impacts the regression of preinvasive breast lesions. Macrophages have recently become an attractive clinical target either through modification of inflammation through use of NSAIDS or fish oil (47,48) or by decreasing macrophages using a variety of targeting agents (13). Unfortunately, initial clinical studies have demonstrated mixed results (13). Our work suggests that targeting macrophages prophylactically may have negative consequences in obese patients. Macrophages, particularly in the context of obesity, are a heterogenous population of cells. A recent study utilizing single cell RNAseq has demonstrated that obese visceral fat contains 7 distinct macrophage populations with potentially different functions and cytokine profiles (49). It is possible that obese mammary adipose tissue will also demonstrate significant heterogeneity in macrophage populations, given the presence of macrophages surrounding crown-like structures within the adipose tissue as well as interacting with the epithelium. However, further studies are necessary to determine how obesity impacts distinct macrophage populations and their activities in other preclinical models of breast cancer subtypes. While we observed increased tumor formation in $p53^{-/-}$ MECs treated during preneoplastic growth in obese mice, depletion of macrophages in obese tumor-bearing mice resulted in abrogated angiogenesis within tumors and diminished tumor growth (50). These results may suggest that the timing of treatment to target macrophage during tumor growth may be a critical consideration in obese patients. Development of new therapeutic strategies to reduce risk of breast cancer in obese women may significantly improve clinical outcomes in this patient population.

Supplementary Material

Refer to Web version on PubMed Central for supplementary material.

ACKNOWLEDGEMENTS

The authors would like to thank Danielle Timm and Brenna Walton for technical assistance. This work was supported by funding from the Susan G. Komen Foundation Career Catalyst Grant CCR1532611(L. M. Arendt). This work was also supported by NIH/NCI grants R01 CA227542 (L. M. Arendt.), F31 CA247265 (G. Kuziel) and University of Wisconsin Carbone Cancer Center Support Grant P30 CA014520, as well as NIH Office of the Director Grants T32 OD010423 (T.Chamberlin) and T35 OD11078 (H.Johnson).

REFERENCES

1. World Health Organization. Obesity and overweight fact sheet. 2016.
2. Reeves GK, Pirie K, Beral V, Green J, Spencer E, Bull D. Cancer incidence and mortality in relation to body mass index in the Million Women Study: cohort study. BMJ 2007;335:1134 [PubMed: 17986716]
3. Chun J, El-Tamer M, Joseph KA, Ditkoff BA, Schnabel F. Predictors of breast cancer development in a high-risk population. Am J Surg 2006;192:474–7 [PubMed: 16978952]
4. Loi S, Milne RL, Friedlander ML, McCredie MR, Giles GG, Hopper JL, et al. Obesity and outcomes in premenopausal and postmenopausal breast cancer. Cancer Epidemiol Biomarkers Prev 2005;14:1686–91 [PubMed: 16030102]
5. Chamberlin T, D'Amato JV, Arendt LM. Obesity reversibly depletes the basal cell population and enhances mammary epithelial cell estrogen receptor alpha expression and progenitor activity. Breast Cancer Res 2017;19:128 [PubMed: 29187227]

6. Lim E, Vaillant F, Wu D, Forrest NC, Pal B, Hart AH, et al. Aberrant luminal progenitors as the candidate target population for basal tumor development in BRCA1 mutation carriers. Nat Med 2009;15:907–13 [PubMed: 19648928]
7. Keller PJ, Arendt LM, Skibinski A, Logvinenko T, Klebba I, Dong S, et al. Defining the cellular precursors to human breast cancer. Proc Natl Acad Sci U S A 2012;109:2772–7 [PubMed: 21940501]
8. Arendt LM, McCready J, Keller PJ, Baker DD, Naber SP, Seewaldt V, et al. Obesity promotes breast cancer by CCL2-mediated macrophage recruitment and angiogenesis. Cancer Res 2013;73:6080–93 [PubMed: 23959857]
9. Gyorki DE, Asselin-Labat ML, van Rooijen N, Lindeman GJ, Visvader JE. Resident macrophages influence stem cell activity in the mammary gland. Breast Cancer Res 2009;11:R62 [PubMed: 19706193]
10. Chakrabarti R, Celia-Terrassa T, Kumar S, Hang X, Wei Y, Choudhury A, et al. Notch ligand Dll1 mediates cross-talk between mammary stem cells and the macrophageal niche. Science 2018;360:eaan4153 [PubMed: 29773667]
11. Carron EC, Homra S, Rosenberg J, Coffelt SB, Kittrell F, Zhang Y, et al. Macrophages promote the progression of premalignant mammary lesions to invasive cancer. Oncotarget 2017;8:50731–46 [PubMed: 28881599]
12. Linde N, Casanova-Acebes M, Sosa MS, Mortha A, Rahman A, Farias E, et al. Macrophages orchestrate breast cancer early dissemination and metastasis. Nat Commun 2018;9:21 [PubMed: 29295986]
13. Brown JM, Recht L, Strober S. The promise of targeting macrophages in cancer therapy. Clin Cancer Res 2017;23:3241–50 [PubMed: 28341752]
14. Network CGA. Comprehensive molecular portraits of human breast tumours. Nature 2012;490:61–70 [PubMed: 23000897]
15. Ochs-Balcom HM, Marian C, Nie J, Brasky TM, Goerlitz DS, Trevisan M, et al. Adiposity is associated with p53 gene mutations in breast cancer. Breast Cancer Res Treat 2015;153:635–45 [PubMed: 26364297]
16. Jerry DJ, Kittrell FS, Kuperwasser C, Laucirica R, Dickinson ES, Bonilla PJ, et al. A mammary-specific model demonstrates the role of the p53 tumor suppressor gene in tumor development. Oncogene 2000;19:1052–8 [PubMed: 10713689]
17. Herschkowitz JI, Simin K, Weigman VJ, Mikaelian I, Usary J, Hu Z, et al. Identification of conserved gene expression features between murine mammary carcinoma models and human breast tumors. Genome Biol 2007;8:R76 [PubMed: 17493263]
18. Medina D, Kittrell FS, Shepard A, Contreras A, Rosen JM, Lydon J. Hormone dependence in premalignant mammary progression. Cancer Res 2003;63:1067–72 [PubMed: 12615724]
19. Tang J, Fernandez-Garcia I, Vijayakumar S, Martinez-Ruis H, Illa-Bochaca I, Nguyen DH, et al. Irradiation of juvenile, but not adult, mammary gland increases stem cell self-renewal and estrogen receptor negative tumors. Stem Cells 2014;32:649–61 [PubMed: 24038768]
20. Wang W, Marinis JM, Beal AM, Savadkar S, Wu Y, Khan M, et al. RIP1 kinase drives macrophage-mediated adaptive immune tolerance in pancreatic cancer. Cancer Cell 2018;34:757–74.e7 [PubMed: 30423296]
21. Yu YR, O'Koren EG, Hotten DF, Kan MJ, Kopin D, Nelson ER, et al. A protocol for the comprehensive flow cytometric analysis of immune cells in normal and inflamed murine non-lymphoid tissues. PLoS One 2016;11:e0150606 [PubMed: 26938654]
22. Jerry DJ, Kittrell FS, Kuperwasser C, Laucirica R, Dickinson ES, Bonilla PJ, et al. A mammary-specific model demonstrates the role of the p53 tumor suppressor gene in tumor development. Oncogene 2000;19:1052–8 [PubMed: 10713689]
23. O'Leary KA, Rugowski DE, Sullivan R, Schuler LA. Prolactin cooperates with loss of p53 to promote claudin-low mammary carcinomas. Oncogene 2014;33:3057–82
24. Tao L, Xiang D, Xie Y, Bronson RT, Li Z. Induced p53 loss in mouse luminal cells causes clonal expansion and development of mammary tumours. Nat Commun 2017;8:14431 [PubMed: 28194015]

25. Subbaramaiah K, Howe LR, Bhardwaj P, Du B, Gravaghi C, Yantiss RK, et al. Obesity is associated with inflammation and elevated aromatase expression in the mouse mammary gland. Cancer Prev Res 2011;4:329–46
26. Seo BR, Bhardwaj P, Choi S, Gonzalez J, Andresen Eguiluz RC, Wang K, et al. Obesity-dependent changes in interstitial ECM mechanics promote breast tumorigenesis. Sci Transl Med 2015;7:301ra130
27. Kratz M, Coats BR, Hisert KB, Hagman D, Mutskov V, Peris E, et al. Metabolic dysfunction drives a mechanistically distinct proinflammatory phenotype in adipose tissue macrophages. Cell Metab 2014;20:614–25 [PubMed: 25242226]
28. Shehata M, Teschendorff A, Sharp G, Novcic N, Russell IA, Avril S, et al. Phenotypic and functional characterisation of the luminal cell hierarchy of the mammary gland. Breast Cancer Res 2012;14:R134 [PubMed: 23088371]
29. Clarke RB, Howell A, Potten CS, Anderson E. Dissociation between steroid receptor expression and cell proliferation in the human breast. Cancer Res 1997;57:4987–91 [PubMed: 9371488]
30. Clarke RB, Spence K, Anderson E, Howell A, Okano H, Potten CS. A putative human breast stem cell population is enriched for steroid receptor-positive cells. Dev Biol 2005;277:443–56 [PubMed: 15617686]
31. Williams AB, Schumacher B. p53 in the DNA-damage-repair process. Cold Spring Harb Perspect Med 2016;6:a026070 [PubMed: 27048304]
32. Wlodarczyk M, Nowicka G. Obesity, DNA damage, and development of obesity-related diseases. Int J Mol Sci 2019;20:1146
33. Mah LJ, El-Osta A, Karagiannis TC. gammaH2AX: a sensitive molecular marker of DNA damage and repair. Leukemia 2010;24:679–86 [PubMed: 20130602]
34. Yoshida K, Yoshida SH, Shimoda C, Morita T. Expression and radiation-induced phosphorylation of histone H2AX in mammalian cells. J Radiat Res 2003;44:47–51 [PubMed: 12841599]
35. MacPhail SH, Banath JP, Yu Y, Chu E, Olive PL. Cell cycle-dependent expression of phosphorylated histone H2AX: reduced expression in unirradiated but not X-irradiated G1-phase cells. Radiat Res 2003;159:759–67 [PubMed: 12751958]
36. Jackson AL, Loeb LA. The contribution of endogenous sources of DNA damage to the multiple mutations in cancer. Mutat Res 2001;477:7–21 [PubMed: 11376682]
37. Valavanidis A, Vlachogianni T, Fiotakis C. 8-hydroxy-2' -deoxyguanosine (8-OHdG): A critical biomarker of oxidative stress and carcinogenesis. J Environ Sci Health C Environ Carcinog Ecotoxicol Rev 2009;27:120–39 [PubMed: 19412858]
38. Carter JM, Hoskin TL, Pena MA, Brahmbhatt R, Winham SJ, Frost MH, et al. Macrophagic "crown-like structures" are associated with an increased risk of breast cancer in benign breast disease. Cancer Prev Res 2018;11:113–9
39. Nelson AC, Machado HL, Schwertfeger KL. Breaking through to the other side: microenvironment contributions to DCIS initiation and progression. J Mammary Gland Biol Neoplasia 2018;23:207–21 [PubMed: 30168075]
40. Binnewies M, Roberts EW, Kersten K, Chan V, Fearon DF, Merad M, et al. Understanding the tumor immune microenvironment (TIME) for effective therapy. Nat Med 2018;24:541–50 [PubMed: 29686425]
41. Stossi F, Madak-Erdogan Z, Katzenellenbogen BS. Macrophage-elicited loss of estrogen receptor-alpha in breast cancer cells via involvement of MAPK and c-Jun at the ESR1 genomic locus. Oncogene 2012;31:1825–34 [PubMed: 21860415]
42. Wang H, Xiang D, Liu B, He A, Randle HJ, Zhang KX, et al. Inadequate DNA damage repair promotes mammary transdifferentiation, leading to BRCA1 breast cancer. Cell 2019;178:135–51.e19 [PubMed: 31251913]
43. Behrend L, Henderson G, Zwacka RM. Reactive oxygen species in oncogenic transformation. Biochem Soc Trans 2003;31:1441–4 [PubMed: 14641084]
44. Rendra E, Riabov V, Mossel DM, Sevastyanova T, Harmsen MC, Kzhyshkowska J. Reactive oxygen species (ROS) in macrophage activation and function in diabetes. Immunobiology 2019;224:242–53 [PubMed: 30739804]

45. Netzer N, Gatterer H, Faulhaber M, Burtscher M, Pramsohler S, Pesta D. Hypoxia, oxidative stress and fat. Biomolecules 2015;5:1143–50 [PubMed: 26061760]

46. Geiger-Maor A, Guedj A, Even-Ram S, Smith Y, Galun E, Rachmilewitz J. Macrophages regulate the systemic response to DNA damage by a cell nonautonomous mechanism. Cancer Res 2015;75:2663–73 [PubMed: 25977329]

47. Fabian CJ, Kimler BF, Hursting SD. Omega-3 fatty acids for breast cancer prevention and survivorship. Breast Cancer Res 2015;17:62 [PubMed: 25936773]

48. Bowers LW, Maximo IX, Brenner AJ, Beeram M, Hursting SD, Price RS, et al. NSAID use reduces breast cancer recurrence in overweight and obese women: role of prostaglandin-aromatase interactions. Cancer Res 2014;74:4446–57 [PubMed: 25125682]

49. Weinstock A, Brown EJ, Garabedian ML, Pena S, Sharma M, Lafaille J, et al. Single-cell RNA sequencing of visceral adipose tissue leukocytes reveals that caloric restriction following obesity promotes the accumulation of a distinct macrophage population with features of phagocytic cells. Immunometabolism 2019;1:e190008 [PubMed: 31396408]

50. Hillers-Ziemer LE, McMahon RQ, Hietpas M, Paderta G, LeBeau J, McCready J, et al. Obesity promotes cooperation of cancer stem-like cells and macrophages to enhance mammary tumor angiogenesis. Cancers 2020;12:502

SIGNIFICANCE

Understanding how obesity impacts early tumor growth and response to macrophage-targeted therapies may improve therapeutics for obese breast cancer patients and identify patient populations that would benefit from macrophage-targeted therapies.

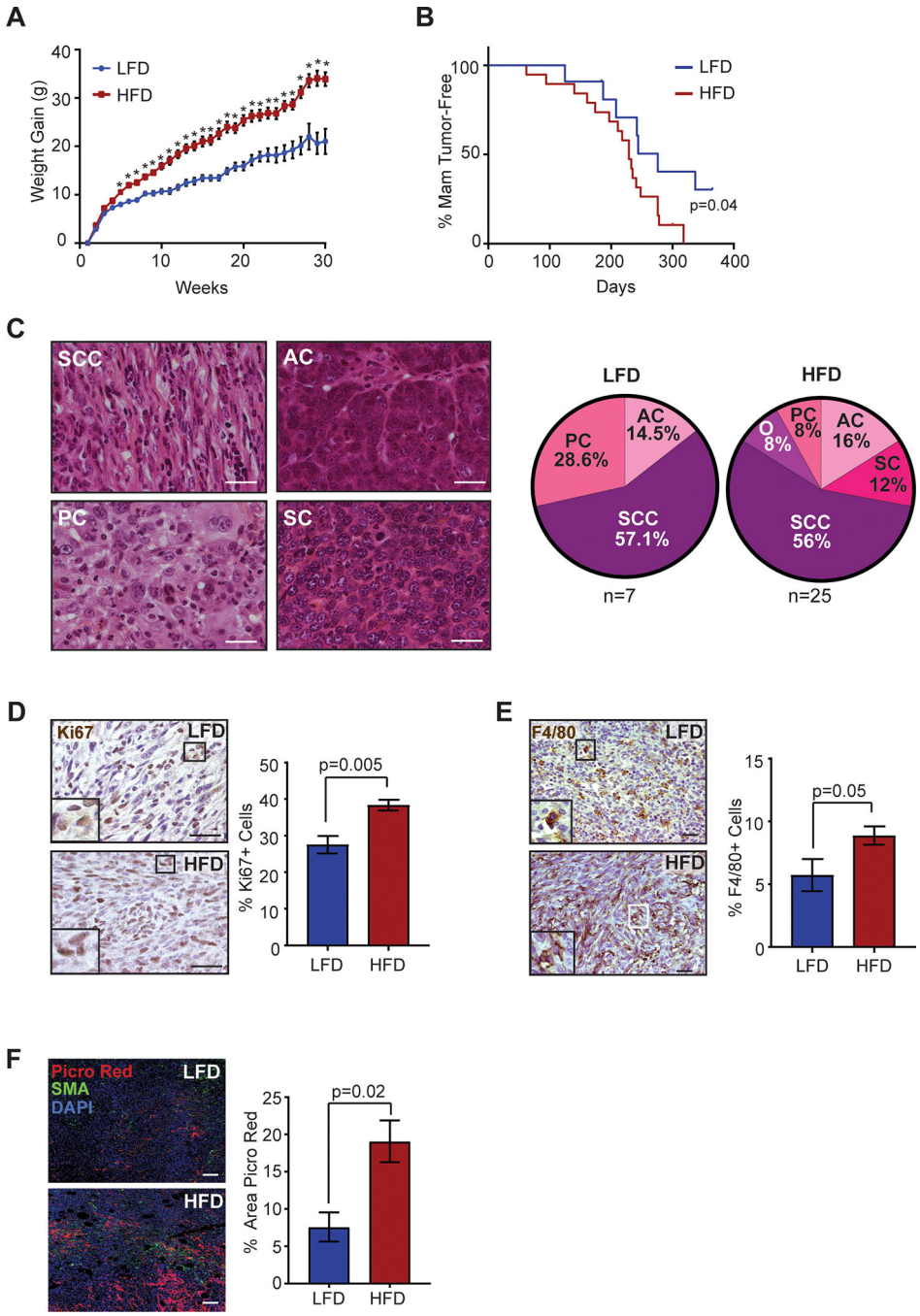

Figure 1.

Obesity increased incidence of $p53^{-/-}$ mammary tumors and enhanced tumor stroma. **A.** $p53^{-/-}$ MEC recipients were fed LFD (n=12) or HFD (n=19) starting at 3 weeks of age (**P*<0.05). **B.** Percent mammary tumor-free survival (*P*=0.04; Kaplan-Meier analysis). **C.** H&E images and distribution of carcinoma histotypes (PC=Pleomorphic carcinoma, AC=Adenocarcinoma, SC=Solid carcinoma, SCC=Spindle cell carcinoma, O=Other). **D.** Percent $Ki67^{+}$ cells in $p53^{-/-}$ carcinomas (n=7 LFD, n=25 HFD). **E.** Percent $F4/80^{+}$ cells in SCC tumors (n=4 LFD, n=13 HFD). **F.** Percent area of picrosirius red stain in mammary

tumors (n=7 LFD, n=19 HFD). Tissue sections were stained for picrosirius red, smooth muscle actin (SMA) and DAPI. Magnification bar=50 μm.

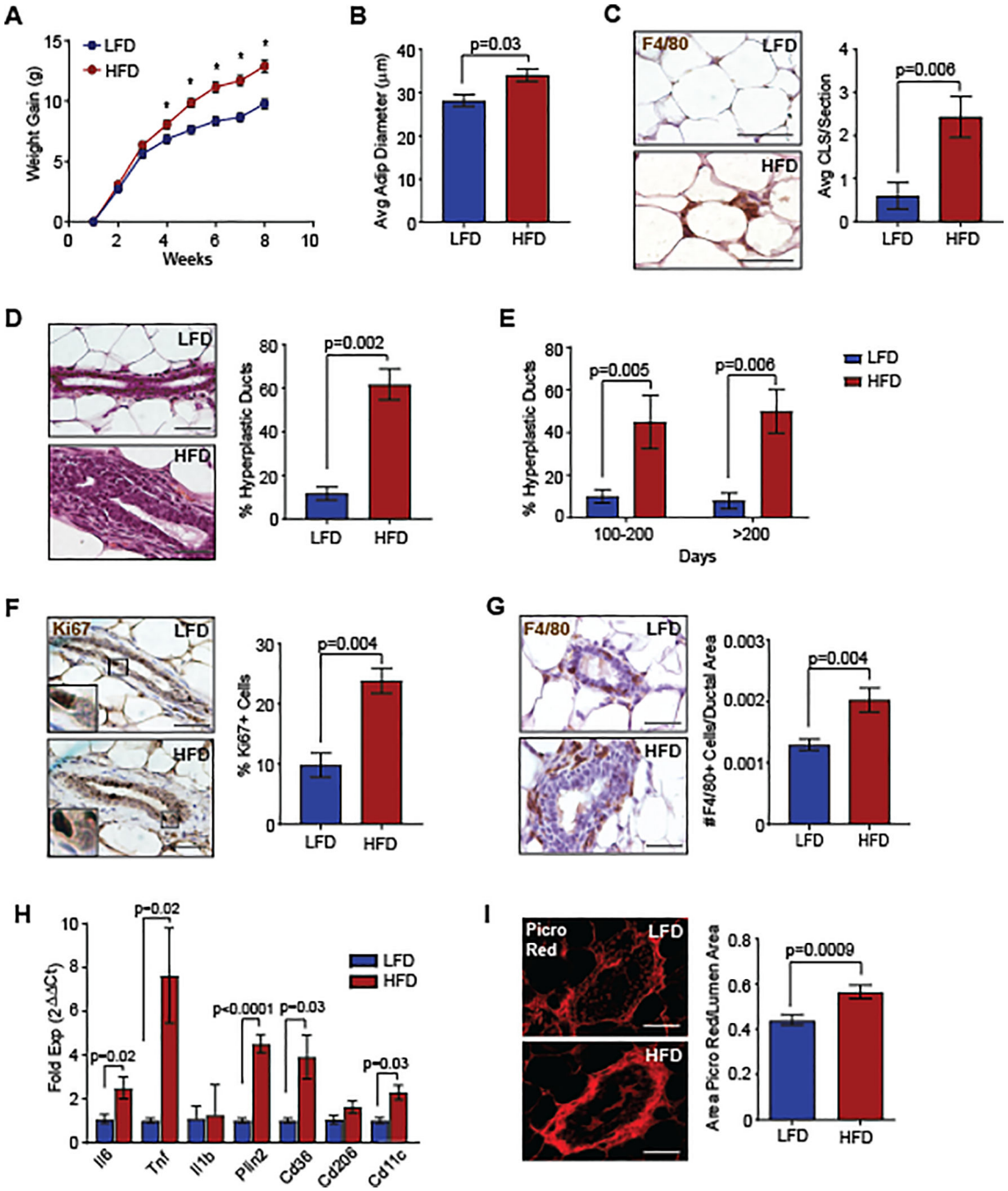

Figure 2.

Obesity enhanced ductal hyperplasia formation with increased macrophage infiltration. **A.** Transplanted mice were fed LFD or HFD (n=20/group, $*P < 0.05$). **B.** Diameters of mammary adipocytes at 8 weeks following transplant (n=5/group). **C.** Crown-like structures (CLS) in mammary glands (n=5/group). **D.** H&E images of ducts in mammary glands 8 weeks following transplant (n=5/group). **E.** Hyperplastic ducts in mammary tissue of non-tumor bearing $p53^{-/-}$ MEC recipients (n=12 LFD, n=14 HFD). **F.** Percent $Ki67^{+}$ cells in hyperplastic ducts (n=5/group). **G.** Number of $F4/80^{+}$ macrophages surrounding mammary

ducts (n=5/group). **H.** Gene expression from F4/80^{+} macrophages isolated from mammary glands (n=5/group). **I.** Picrosirius red stain surrounding mammary ducts (n=5/group). Magnification bar=50 μm.

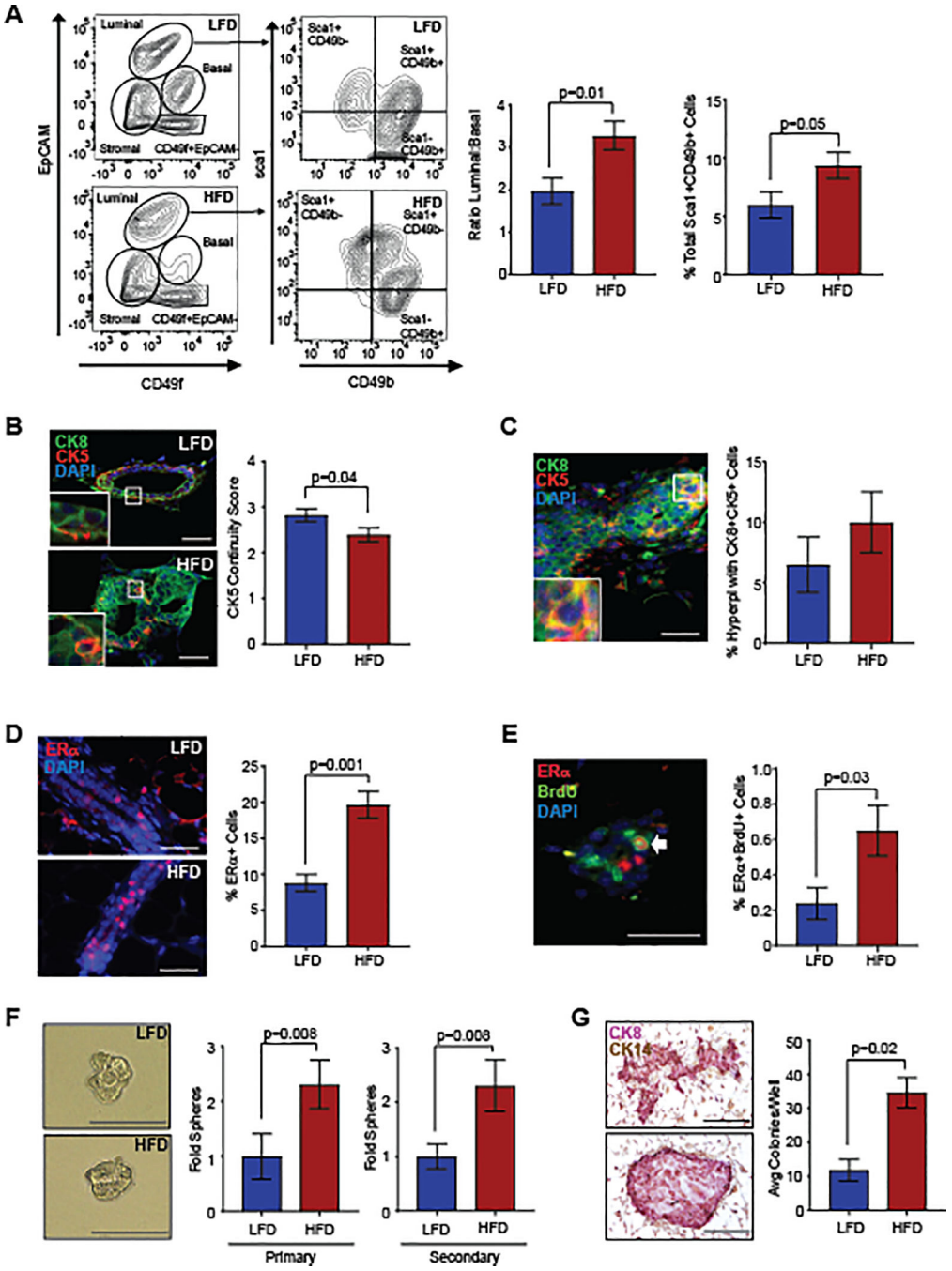

Figure 3.

Obesity increased $p53^{-/-}$ MEC stem/progenitor activity 8 weeks following transplant. **A.** Representative contour plots depict gates for luminal cells ($EpCAM^{hi}CD49f^{lo}$) and basal cells ($EpCAM^{lo}CD49f^{hi}$). Luminal cells were also gated by expression of Sca-1 and CD49b (n=9/group). **B.** Continuity of $CK5^{+}$ basal cells surrounding $CK8^{+}$ luminal cells (n=5/group). **C.** MECs expressing both CK8 and CK5 (yellow). **D.** Percent $ER\alpha^{+}$ MECs in mammary ducts (n=5/group). **E.** Percent of MECs co-labeled for ERα and BrdU (n=5/group). **F.** Isolated MECs were plated to form primary and secondary mammospheres (n=5–

6/group). **G.** MEC colonies expressed CK8 and CK14 (n=5–6/group). Magnification bar=50 μm.

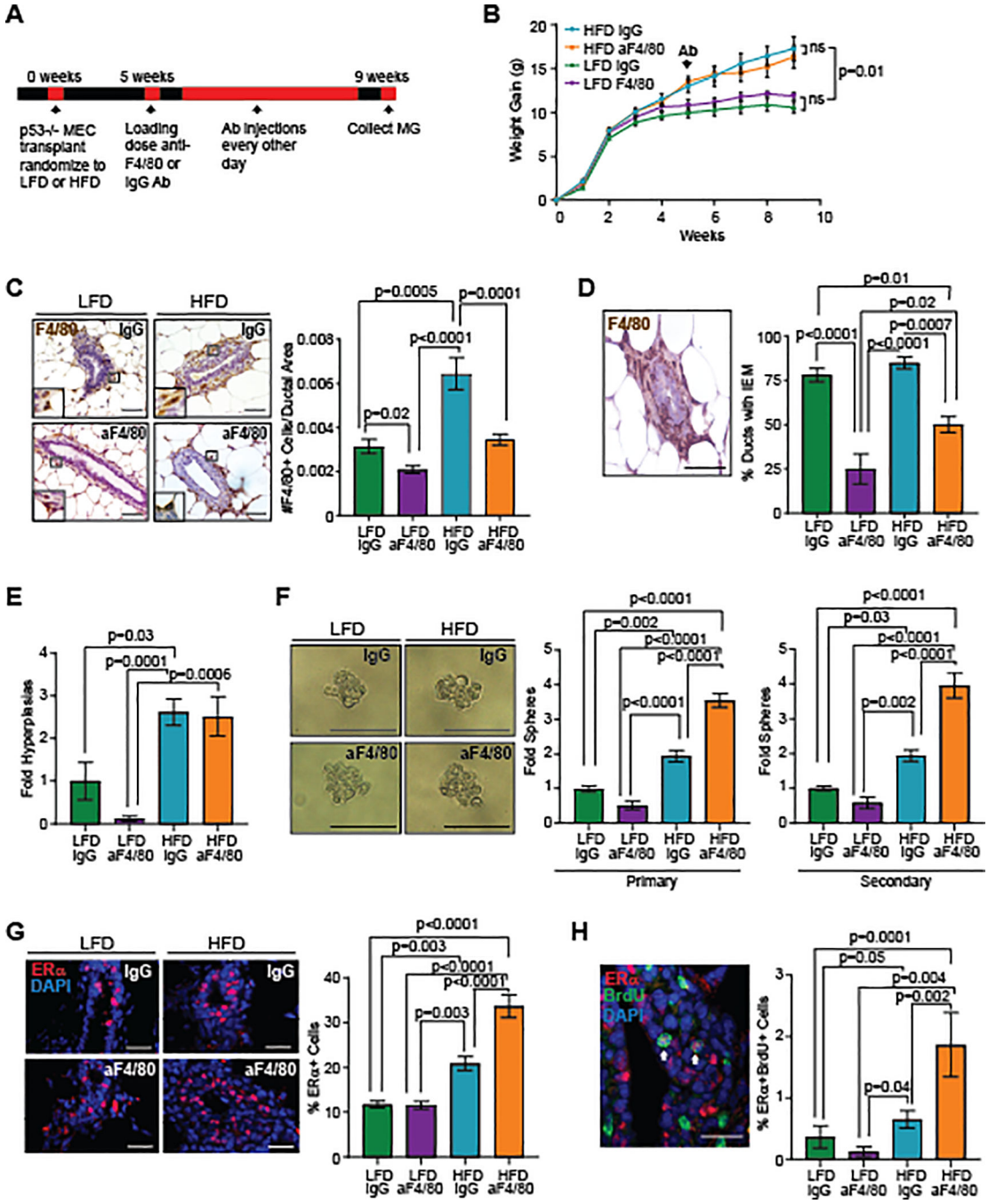

Figure 4.

Depletion of macrophages enhanced p53$^{-/-}$ stem/progenitor cell activity in obesity. **A.** Schematic of macrophage depletion experiment. **B.** Transplant recipients were fed LFD or HFD starting at 3 weeks of age and treated with IgG or aF4/80 antibodies (n=8/LFD group and n=9/HFD group). **C.** F4/80^{+} macrophages surrounding mammary ducts (n=3/LFD group, n=4/HFD group). **D.** Percentage of ducts containing interepithelial macrophages (IEM) (n=3/LFD group, n=4/HFD group). **E.** Fold change of hyperplastic ducts (n=3/LFD group, n=4/HFD group). **F.** MECs from recipients formed primary and secondary

mammospheres (n=5/group). **G.** Percentage of ERα+ MECs (n=3/LFD group, n=4/HFD group). **H.** Percent of MECs co-labeled for ERα and BrdU (n=3/LFD group, n=4/HFD group). Magnification bar=50 μm.

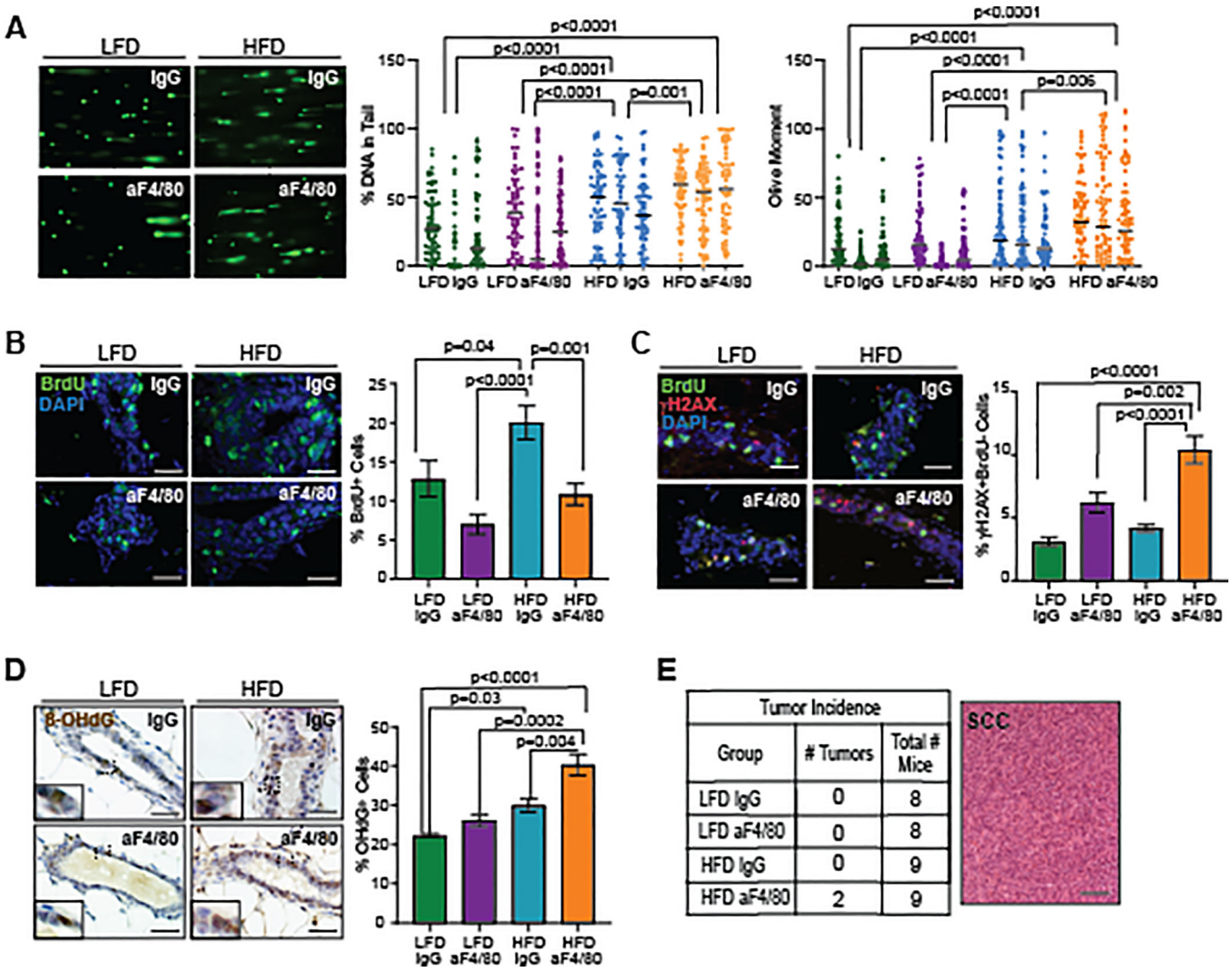

Figure 5.

Macrophage depletion in obese mice led to increased $p53^{-/-}$ MECs with DNA damage. **A.** Representative comet assays from $p53^{-/-}$ MECs. Percent DNA in tail and olive moment were quantified from 50 cells/recipient (n=3/group; Kruskal-Wallis test with Dunn's multiple comparison post-test). Bars represent geometric means. **B.** Percent of $BrdU^{+}$ MECs (n=3–4/group). **C.** Percent of MECs labeled for γH2AX and BrdU (n=3–4/ group). **D.** Percent of MECs labeled for 8-OHdG (n=3–4/group). **E.** Tumor incidence and image of $p53^{-/-}$ spindle cell carcinomas that formed in aF4/80-treated HFD-fed mice (P=0.06, chi-squared test for trend). Magnification bar=50 μm.